JCTC Journal of Chemical Theory and Computation

Solute Partitioning into Lipid Bilayers: An Implicit Model for Nonuniform and Ordered Environment

Giulia Parisio and Alberta Ferrarini*

Dipartimento di Scienze Chimiche, Università degli Studi di Padova Via Marzolo, 1 - 35131 Padova, Italy

Received April 26, 2010

Abstract: We have developed a theoretical and computational methodology to evaluate the coupled orientational−positional distribution of solutes in lipid bilayers. Four different contributions to the solute free energy are considered, which can be traced back to (i) electrostatic and (ii) dispersion interactions between the solute and environment, (iii) work for the formation of a solute-shaped cavity, and (iv) anisotropic interactions with the ordered acyl chains. An atomistic representation of the solute is adopted, which includes the conformational degrees of freedom, whereas an implicit model is used for the water/bilayer environment. The highly nonuniform and anisotropic nature of this is introduced through the profiles of density, dielectric permittivity, lateral pressure, and acyl chain order parameters, which can be derived from experiments or simulations. Effects of chemical composition and physical state of the bilayer can be accounted for by a proper form of these profiles. The methodology which we propose is suitable for the integrated calculation of spectroscopic observables for probes in membranes, for the estimate of partition and permeability coefficients of solutes, and for the implicit modeling of the membrane environment in molecular dynamics and Monte Carlo simulations. Here, the method is presented, and the underlying assumptions are discussed. Cholesterol in the liquid crystalline DPPC bilayer is taken as a case study, to illustrate the capabilities of the proposed approach. Free energy maps, distribution profiles, and orientational properties are shown; they compare well with those obtained from all-atom molecular dynamics simulations, as well as with available experimental data, suggesting that the model used is able to capture the subtle effects of the interplay between intermolecular interaction and nanoscale architecture of the lipid bilayer. The detailed picture provided by our calculations appears suitable to investigate the determinants of the behavior of solutes in lipid membranes, highlighting even nonstraightforward issues, which may have biophysical implications.

Introduction

Partitioning of solutes into lipid bilayers has important implications: beside playing a role in cellular processes, it underlies the permeation of drugs across biomembranes. This has motivated along the years a steady effort to develop models able to catch the features of the membrane environment.[1] Traditionally, lipid bilayers have been approximated as slabs of apolar solvents in water, and their high nonuniformity and orientational order have been neglected.[2] Actually, these are the most peculiar features of lipid bilayers, which are characterized by depth-dependent anisotropic stresses and by enormous gradients of properties over a nanometer length scale. The profiles of density, lateral forces, and order are strictly related to the lipid composition and the physical state of the bilayer: they depend on the acyl chain saturation and the headgroup structure and exhibit significant differences between the liquid crystal and the gel phase. The importance of these aspects was recognized early by Dill and co-workers, who singled out the peculiar nature

* Corresponding author phone: +39 049 8275682; fax: +39 049 8275239; e-mail: alberta.ferrarini@unipd.it.

10.1021/ct100210u
Published on Web 07/06/2010

of partitioning when "interfacial phases" are involved.[3,4] However, the structural features of lipid bilayers were generally ignored in subsequent studies, most of which focused on the effects of the dielectric discontinuity and tried to extend to its description the theoretical and computational methods developed for liquid solvents.[5−7] The introduction of bilayer properties into solvation theories is a difficult task: due to the inherent chemical and structural complexity, modeling of bilayers remains a challenge for statistical theories of liquids.[8,9] Only in a few exceptions were the structural features of the bilayer included in models for solute partitioning between water and lipid membranes. Xiang and Anderson evaluated the free energy change upon formation of a molecular cavity in the bilayer as the reversible work against the lateral pressure, including in this way the configurational entropy and the change in conformational energy of lipid chains.[10] They performed calculations for ellipsoidal solutes, with a lateral pressure profile obtained from coarse-grained molecular dynamics simulations, and could predict the dependence of solute orientational order parameters on the molecular volume and on the ratio of the long to short molecular axis. Mitragotri and co-workers developed a model for the cavity work for ellipsoidal solutes in the ordered chain region.[11] It was based on a 2D form of scaled particle theory and related partition coefficients to solute size and bilayer properties, like lipid density and lipid chain order parameters. Kessel and co-workers assumed a decomposition of the solute-bilayer interaction free energy in a set of contributions including, in addition to electrostatic and nonpolar terms, customary in solvation theories, two further terms accounting for elastic deformations of the bilayer and conformational restrictions of lipid chains induced by the solute.[12] The former contributions were described by continuum solvent models with atomistic representation of the solute. For the latter, the elastic continuum theory and a liquid crystal model, respectively, were used, and for simplicity, the solute was represented as a cylinder.

We present here a theoretical and computational method for modeling the free energy landscape of solutes in lipid bilayers, wherein the order and nonuniformity characteristics of this environment are consistently taken into account. The free energy of solutes is expressed as the superposition of the work required to form a molecular shaped cavity and other contributions associated with the switching on of solute−solvent interactions. The cavity work is evaluated on the basis of the lateral pressure profile.[13] A nonpolar and an electrostatic contribution are evaluated as a function of the density and permittivity gradients in the bilayer,[14] respectively; a further term, explicitly accounting for the anisotropy of intermolecular interactions due to lipid chain order, is derived from liquid crystal theory.[15] The environment enters with its collective properties: dielectric permittivity, lateral pressure, and density profile, in addition to acyl chain order parameters. Values appropriate for the physical state and composition of the bilayer can be obtained from molecular dynamics simulations or from experiments. An atomistic representation of the solute is used, comprising its geometry, charge distribution, polarizability, and flexibility. Free energy maps are obtained as a function of molecular position and orientation, whose coupling is intrinsic to the bilayer structure.

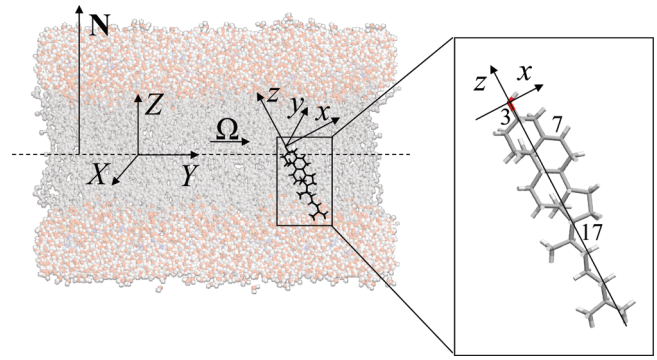

Figure 1. Cholesterol and DPPC bilayer, with the bilayer and the molecular reference frames, (*X*,*Y*,*Z*) and (*x*,*y*,*z*), respectively. The laboratory frame has its origin in the bilayer midplane and the *Z* axis parallel to the bilayer normal (**N**); the latter is directed from the midplane toward water. The molecular frame has its origin at the nuclear position of the oxygen atom and the *x*, *y*, and *z* axes anchored to the fused ring core, with the *z* axis parallel to the C_3-C_{17} segment and the *x* axis coplanar with C_7 (atom numbering as in Figure S5, Supporting Information). The Euler angles $\Omega = (\alpha, \beta, \gamma)$ specify the orientation of the molecular frame with respect to the laboratory frame.

In the next section, the theoretical model is presented. First, the different contributions to the solute free energy are described; then suitable distribution functions and average values are introduced. In the third section, computational details are reported. In the fourth section, cholesterol in liquid crystalline DPPC (1,2-dipalmitoyl-*sn*-glycero-3-phosphatidylcholine; see Abbreviations) is taken as an example to illustrate the features of the proposed methodology. The results are discussed in relation to experimental data and other theoretical−computational investigations. In the final section, capabilities and limits of the proposed approach are summarized, and future developments are outlined.

Theory

The lipid organization in the bilayer defines an alignment axis, the so-called director (**n**), which in the liquid crystal phase is parallel to the bilayer normal (**N**). So, the degrees of freedom of a rigid solute within the lipid bilayer are its position along the normal and its orientation with respect to it; the former is defined, in the bilayer frame, by the *Z* coordinate of the origin of the molecular frame, the latter by the Euler angles, $\Omega = (\alpha, \beta, \gamma)$, which specify the orientation of the molecular frame in the bilayer frame. (Actually, due to the axial symmetry of the environment, the *X*, *Y* coordinates of the origin of the molecular frame, as well as the Euler angle α, do not need to be specified.) Reference frames and transformations are sketched in Figure 1. Our implicit model assumes that the solute positional and orientational distribution is determined by a mean field potential $U(\Omega,Z)$: this can be viewed as the energy of the "solute microstate" (Ω,Z) in the solvent, under the implicit assumption that all degrees of freedom of the latter are averaged out, which gives $U(\Omega,Z)$ a free energy character.

As customary in solvation models,[16] we decompose the mean field potential experienced by a solute into a set of contributions:

$$U = U_{cav} + U_{el} + U_{disp} + U_{ord} \quad (1)$$

The first term, U_{cav}, is related to the work required to form a molecular cavity in the medium, whereas the next two terms, U_{el} and U_{disp}, account for the switching on of electrostatic and dispersion interactions between the solute and environment, respectively. In addition to these terms, which usually appear in solvation models, we have included a further contribution, U_{ord}, which can be traced back to the anisotropy of intermolecular interactions, due to acyl chain order, in the bilayer environment. In the following, the individual contributions to the mean field potential will be considered, and the model adopted for each of them will be presented.

Cavity Work. The cavity contribution to the mean field potential is evaluated as the work against the external pressure to create a cavity containing the solute. As a consequence of the system organization, an axially symmetric pressure tensor can be defined in liquid crystalline bilayers; one of its components, the normal pressure P_N, is parallel to the normal and everywhere equal to the bulk water pressure, whereas the other component, the lateral pressure P_L, is a function of depth, due to the position dependence of forces in the interior of the bilayer. The difference $\pi(Z) = P_L(Z) - P_N$, generally denoted as the lateral pressure profile, is identified with the opposite of a surface tension and describes the local tendency of the bilayer to contract, becoming thicker ($P_L - P_N < 0$), or to expand, becoming thinner ($P_L - P_N > 0$).[13,17–19] Though not easily measurable, the lateral pressure profile across a lipid bilayer can be calculated. General forms can be derived by statistical-thermodynamics models,[9] whereas more specific profiles can be obtained from atomistic simulations.[20] The lateral pressure should be intended as a force per unit area perpendicular to the bilayer plane and varies dramatically with the position across the bilayer, ranging from very high positive to very low negative values within a few nanometers. Three regions are generally identified: (1) the hydrophilic headgroup region, where $P_L > 0$ due to electrostatic and steric interactions and hydration repulsion; (2) the membrane−water interface, where $P_L < 0$ as a consequence of the tendency to decrease the lipid−water interfacial area; and (3) the bilayer interior, where again $P_L > 0$, due to steric repulsions between hydrophobic chains. The stability of the bilayer is determined by the balance of these contributions. The lateral pressure profile is a specific property of the bilayer, which depends on its chemical composition and physical state.[20,21] The integral of the lateral pressure profile across a monolayer is equal to the opposite of its surface tension.[22] In a tensionless bilayer, the surface tension vanishes: repulsion in hydrophobic and hydrophilic regions, mainly due to short-range lipid−lipid interactions and headgroup hydration, is balanced by cohesion, ascribed to the hydrophobic effect, at the hydrophobic/hydrophilic interface. The first moment of the lateral pressure profile is related to the bending elastic modulus and the second moment to the saddle splay modulus.[23–25]

The work required to create a molecular shaped cavity containing a solute at the position Z with orientation Ω is calculated as the integral:[13]

$$U_{cav}(\Omega, Z) = \int_{\text{cavity length}} P_L(Z + z')\, \sigma(\Omega, Z + z')\, dz' \quad (2)$$

where $\sigma(\Omega,Z + z')$ is the surface area of the section of the cavity at the coordinate $(Z+z')$ in the bilayer frame and the integral is over the length of the cavity, along the z' axis of a molecular frame parallel to the bilayer frame, with its origin in Z. $P_L(Z+z')$ is the lateral pressure at the same coordinate $(Z+z')$; in water, it takes a constant value, equal to bulk pressure. Thus, changes in the sign of the lateral pressure inside the bilayer correspond to regions where solute insertion is favorable ($P_L < 0$, i.e., attractive interactions in the bilayer) and unfavorable ($P_L > 0$, i.e., repulsive interactions in the bilayer).

Electrostatic Interactions. The electrostatic contribution to the mean field potential is the work required to charge the solute in its environment. Within the continuum approximation, the molecule is treated as an assembly of charges in a low dielectric molecular cavity embedded in a dielectric medium, and the electrostatic free energy is then evaluated by solving the Poisson equation.[26,27] Approximate expressions for the electrostatic free energy are provided by the so-called generalized Born models.[28,29] They can account for the chemical structure of the solute at a low computational cost, which may be important when repeated calculations must be performed, as is our case, since several solute positions and orientations must be sampled. A difficulty in the case of bilayers derives from the nanoscale nonuniformity, which makes the definition of the dielectric permittivity not obvious.[30] Forms suitable for the membrane environment have been proposed.[31–36] In the approach developed by Tanizaki and Feig, the phospholipid bilayer is modeled as a multilayer composed of a small number of dielectric slabs.[14] When the molecular charge distribution is described as a set of atomic charges located at the nuclear positions, the electrostatic free energy of the solute, in the Ω orientation at the Z position along the bilayer normal, is expressed as

$$U_{el}(\Omega, Z) = -\frac{1}{2}\sum_{i=1}^{N}\sum_{j=1}^{N}\left(\frac{1}{\varepsilon_{in}} - \frac{1}{\dfrac{\varepsilon^i_{out}(Z_i) + \varepsilon^j_{out}(Z_j)}{2}}\right) \frac{q_i q_j}{\sqrt{r_{ij}^2 + R_i^B R_j^B \exp(-r_{ij}^2/F R_i^B R_j^B)}} \quad (3)$$

where summations are extended to all solute atoms (N), q_i is the atomic charge of the ith atom at the position Z_i, $\varepsilon^i_{out}(Z_i)$ is the local solvent (outer) dielectric constant defined on the basis of the ith atom van der Waals radius,[14] ε_{in} is the solute (internal) dielectric constant, r_{ij} is the distance between the ith and the jth charges, F is an empirical parameter, and R_i^B is the effective Born radius of the ith atom. This is calculated as

$$R_i^{\mathrm{B}} = \frac{1}{C_0 A_{4i} + C_1\left(\frac{3\varepsilon_{\mathrm{out}}(Z_i)}{3\varepsilon_{\mathrm{out}}(Z_i) + 2\varepsilon_{\mathrm{in}}}\right)A_{7i}} + D + \frac{E}{\varepsilon_{\mathrm{out}}(Z_i) + 1} \tag{4}$$

where C_0, C_1, D, and E are empirical parameters and A_{4i} and A_{7i} are atom specific quantities defined as

$$A_{ni} = \left(\frac{1}{(n-3)(R_i^{\mathrm{vdW}})^{n-3}} - \frac{1}{4\pi}\int_{\substack{\text{molecular}\\ \text{volume}\\ r'>R_i^{\mathrm{vdW}}}} \frac{1}{r'^n}\,\mathrm{d}\mathbf{r}'\right)^{1/(n-3)} \tag{5}$$

with R_i^{vdW} being the van der Waals radius of the ith atom.

Dispersion Interactions. The dispersion contribution to the mean field potential is evaluated on the basis of the London expression, which for a pair of polarizable spherical particles, i and j, with volume polarizabilities α_i and α_j, reads $U_{ij}^{\mathrm{disp}} = -^3/_4 I(\alpha_i\alpha_j)/(r_{ij}{}^6)$. Here, r_{ij} is the distance between the centers of the spheres and I is the ionization potential, which is assumed to be equal for the two particles. We represent solute and solvent molecules as assemblies of polarizable spheres and introduce the solvent nonuniformity through the position-dependent density of its components; thus, the dispersion contribution to the solvation free energy of an arbitrary solute in the Ω orientation at the Z position along the bilayer normal is calculated as

$$U_{\mathrm{disp}}(\Omega, Z) = -\frac{3}{4} I \sum_{i=1}^{N}\alpha_i \sum_{j=1}^{M}\alpha_j \int_{\substack{\text{solvent}\\ r'>R_i^{\mathrm{d}}+R_j^{\mathrm{vdW}}}} \frac{\rho_j(Z_i + z')}{r'^6}\,\mathrm{d}\mathbf{r}' \tag{6}$$

where N is the number of atoms in the solute and M is the number of polarizable units in the solvent. A coarse-grained representation of this has been used, whose details are reported in Figure S2 (Supporting Information). The integral extends over the whole solvent volume outside a sphere centered on the ith solute atom, with a radius equal to the sum of an effective radius (R_i^{d}) and the van der Waals radius of the jth solvent component (R_j^{vdW}); $\mathbf{r}' = (x',y',z')$ is a vector position in a local frame, parallel to the bilayer frame, with its origin in the center of the ith atom, located at Z_i in the bilayer frame. In the integral, ρ_j is the number density of the jth polarizable unit of solvent, which is a function of the position along the bilayer normal, defined by the sum $Z_i + z'$. The atomic effective radius R_i^{d} is defined as[37]

$$R_i^{\mathrm{d}} = 1/\sqrt[3]{3}A_{6i} \tag{7}$$

with A_{6i} calculated according to eq 5.

Anisotropic Interactions with Acyl Chains. The contributions to the mean field potential considered so far retain the nonuniformity of the lipid bilayer but neglect the presence of orientational order in the lipid chain region. In the liquid crystal phase, chains are preferentially aligned along an axis (the director **n**), which coincides with the normal **N**, and all properties are axially symmetric with respect to this axis. The degree of alignment is quantified by the chain order parameters, S_{CD}^i, which take their name from the fact that they are obtained from NMR quadrupole splittings for deuteriated acyl chains.[38] They are defined as

$$S_{\mathrm{CD}}^i = \frac{3\langle\cos^2\theta_i\rangle - 1}{2} \tag{8}$$

where θ_i is the angle between the C_iD bond and the bilayer normal (see Figure S1, Supporting Information); the angular bracket denotes a statistical average. If acyl chains were perfectly aligned to the bilayer normal in the all-*trans* conformation, S_{CD}^i would be equal to -0.5 for any i; for randomly oriented chains (as in isotropic liquids), S_{CD}^i would vanish for any i. The S_{CD}^i order parameters are generally negative, since the C_iD bonds preferentially lie perpendicular to the bilayer normal. They exhibit typical profiles, which depend on the phospholipid structure and the physical state of the system; for saturated lipids, $|S_{\mathrm{CD}}^i|$ decreases from relatively high values close to the headgroup to small values on moving toward the chain end.[38]

As a consequence of the chain order, anisotropic interactions are not totally washed out by the orientational average in the bilayer environment. It is important to realize that the interactions which we are considering here have axial symmetry, resulting from the partial alignment of chain segments, though they do not have the polar character originated by the presence of an interface. A related property is birefringence of lipid bilayers; the refractive index parallel to the bilayer normal (n_{e}) is higher than the perpendicular one (n_{o}),[39,40] which means that the average polarizability is higher perpendicular than parallel to the bilayer. To account for the anisotropy of the interactions of solutes with acyl chains, we have extended to bilayers a model which was originally proposed for thermotropic nematic liquid crystals.[15] This is a phenomenological molecular field model which has been proven to be able to capture the relation between molecular structure and orientational order in nematics and has been successfully used to predict the dependence on molecular structure of diverse properties of nematic liquid crystals.[41−43] The model, which can be considered an extension of the Maier−Saupe theory[44] allowing for the account of the molecular shape, bases on the assumption that each element of the surface of a molecule in the nematic phase (of symmetry $D_{\infty h}$) preferentially aligns to the director. The orienting potential, dU_{ord}, acting on each infinitesimal element dS of the molecular surface, is a function of the angle θ between its normal **s** and the director **n** and can be expanded on the basis of Legendre polynomials.[45] Given the symmetry of the system, the first nonvanishing term of this expansion is proportional to the second Legendre polynomial, thus

$$dU_{\mathrm{ord}} = k_{\mathrm{B}}T\xi P_2(\cos\theta)dS \tag{9}$$

where k_{B} is the Boltzmann constant, T is the temperature, and ξ a positive parameter, which quantifies the orienting strength of the environment; it depends on the degree of orientational order and vanishes in the isotropic phase. The overall orienting potential experienced by a molecule in the nematic phase is then obtained by integrating eq 9 over the molecular surface, S:

$$U_{ord}(\Omega) = k_B T \xi \int_S P_2(\cos\theta)\, dS \quad (10)$$

It can be easily seen that, in the model case of a cylindrical particle with lateral area S_{cyl}, the Maier−Saupe form[44] is recovered, $U_{ord}(\beta) = -c_2 P_2(\cos\beta)$, where β is the angle between the cylinder axis and nematic director and $c_2 = k_B T \xi S_{cyl}/2$:[46] the particle preferentially orients with its axis along the nematic director, with no distinction between parallel and antiparallel orientation. According to the molecular field theory, the orienting strength can be related to the order parameters of the nematic phase;[47] if mesogens are approximated as cylindrical particles, the relationship $\xi \propto \langle P_2 \rangle$ holds, where $\langle P_2 \rangle$ is the second rank order parameter, which specifies the degree of order of cylinders.[15] It may be worth remarking that the mean field potential, eq 10, is experienced by all molecules in the nematic system, both mesogens and solutes, if present. The specific form of this potential will depend on the molecular structure, through the molecular surface. On the contrary, the orienting strength ζ is a phase property; at a low concentration of solutes, it is nearly the same as for the pure nematic solvent and is proportional to solvent order parameters.

Extension of the model to lipid bilayers requires the introduction of a position-dependent orienting strength, $\xi = \xi(Z)$; so the orienting contribution to the mean field potential experienced by a solute in a lipid bilayer is expressed as

$$U_{ord}(Z, \Omega) = k_B T \int_S \xi(Z + z') P_2(\cos\theta)\, dS \quad (11)$$

where z' is the position of the surface element dS along an axis parallel to the normal **N**, in a molecular frame parallel to the bilayer frame, with its origin in Z. The profile of the orienting strength, $\xi(Z)$ is a specific function of the bilayer, which depends on the lipid composition and temperature. Extending to the bilayer the same considerations valid for nematics, we can assume a linear relationship between orienting strength ξ and S^i_{CD} order parameters: the orienting strength at the coordinate $\langle Z_i \rangle$, equal to the average position, along the bilayer normal, of the C_i atom, is expressed as $\xi(\langle Z_i \rangle) = -(A/k_B T) S^i_{CD}$, where A is a positive constant. Given the S^i_{CD} order parameters, which are available from experiments or simulations, the values of A and $\langle Z_i \rangle$ can be determined as explained in the Supporting Information.

Density Probability for Solute Position and Orientation. For any molecular position along the bilayer normal and any molecular orientation in the bilayer frame of reference, the mean field potential $U(\Omega,Z)$ is calculated as the sum of the contributions expressed by eqs 2, 3, 6, and 11. Under the conditions of the canonical ensemble, the coupled positional-orientational distribution function can then be calculated as

$$P(\Omega, Z) = \frac{\exp(-U(\Omega, Z)/k_B T)}{Q} \quad (12)$$

with the partition function

$$Q = \int_0^L dZ \int \exp(-U(\Omega, Z)/k_B T)\, d\Omega \quad (13)$$

where T is the temperature, k_B is the Boltzmann constant, and $\int ... d\Omega = \int_0^{2\pi} d\gamma \int_0^{\pi} ... \sin\beta\, d\beta$. The normalization condition $\int_0^L dZ \int P(\Omega,Z)\, d\Omega = 1$ holds. The integral over the Z variable is taken over the bilayer half-thickness, under the assumption that the midplane is a symmetry plane. The upper integration limit, L, depends on the system under investigation. For the calculation of all those properties which only depend on the solute behavior within the bilayer, but are unaffected by the relative amount of solute in the water and bilayer, we can take as a reasonable choice for L a value large enough to ensure that for $Z = L$ the solute behavior can be assumed to be the same as in bulk water.

We can then define the reduced probability distribution function:

$$P_\Omega(Z) = \frac{Q_\Omega(Z)}{Q} \quad (14)$$

where the orientational partition function is defined as

$$Q_\Omega(Z) = \int \exp(-U(\Omega, Z)/k_B T)\, d\Omega \quad (15)$$

so that the normalization condition $\int_0^L P_\Omega(Z)\, dZ = 1$ holds. The reduced distribution function $P_\Omega(Z)$ can be expressed in the Boltzmann form:

$$P_\Omega(Z) = \frac{\exp(-u(Z)/k_B T)}{\int_0^L \exp(-u(Z)/k_B T)\, dZ} \quad (16)$$

with

$$u(Z) = \text{const} - k_B T \ln Q_\Omega(Z) \quad (17)$$

which can be interpreted as the transfer free energy of the solute from water to the position Z in the bilayer, if the constant is taken equal to the value of $k_B T \ln Q_\Omega$ in bulk water.

Once the coupled positional-orientational distribution is known, the average value $\langle f \rangle$ of any arbitrary function $f(\Omega,Z)$ is defined as

$$\langle f \rangle = \int_0^L dZ \int f(\Omega, Z)\, P(\Omega, Z)\, d\Omega \quad (18)$$

Partially averaged functions may also be meaningful; for instance, the orientationally averaged value of the function $f(\Omega,Z)$ can be calculated as

$$\langle f \rangle_\Omega(Z) = \frac{1}{P_\Omega(Z)} \int f(\Omega, Z)\, P(\Omega, Z)\, d\Omega \quad (19)$$

Distribution Functions for Flexible Solutes. The model can be easily extended to flexible solutes. Let us denote as χ the torsional degrees of freedom of the solute; then, the mean field potential, eq 1, will become a function of the molecular conformation, $U(\Omega,Z,\chi)$. If $V(\chi)$ is the torsional potential of the molecule in a vacuum, the coupled orientational-positional-torsional density probability of the solute is defined as

$$P(\Omega, Z, \chi) = \frac{\exp(-V(\chi)/k_BT)\exp(-U(\Omega, Z, \chi)/k_BT)}{Q} \quad (20)$$

with the partition function

$$Q = \int_0^L dZ \int d\Omega \int \exp(-V(\chi)/k_BT)\exp(-U(\Omega, Z, \chi)/k_BT)\, d\chi \quad (21)$$

and the normalization condition $\int_0^L dZ \int d\Omega \int P(\Omega,Z,\chi)\, d\chi = 1$.

In analogy with what is shown above, we can define a reduced position distribution function $P_{\Omega,\chi}(Z)$:

$$P_{\Omega,\chi}(Z) = \frac{Q_{\Omega,\chi}(Z)}{Q} \quad (22)$$

with

$$Q_{\Omega,\chi}(Z) = \int d\Omega \int \exp(-V(\chi)/k_BT)\exp(-U(\Omega, Z, \chi)/k_BT)\, d\chi \quad (23)$$

and the normalization condition $\int_0^L P_{\Omega,\chi}(Z)\, dZ = 1$. In analogy with eq 17, we can define the free energy:

$$u(Z) = \text{const} - k_BT \ln Q_{\Omega,\chi}(Z) \quad (24)$$

which includes entropic effects deriving from rotational and torsional restrictions in the bilayer environment.

The effect of the environment on the conformational distribution can be analyzed in terms of the reduced conformational distribution functions, obtained by averaging over the orientational and positional degrees of freedom:

$$P_{\Omega,Z}(\chi) = \frac{Q_{\Omega,Z}(\chi)}{Q} \quad (25)$$

with

$$Q_{\Omega,Z}(Z, \chi) = \exp(-V(\chi)/k_BT) \int_0^L dZ \int e^{-U(\Omega,Z,\chi)/k_BT} d\Omega \quad (26)$$

and the normalization condition $\int P_{\Omega,Z}(\chi) d\chi = 1$. Equation 25 can also be expressed as:

$$P_{\Omega,Z}(\chi) = \frac{\exp(-V'(\chi)/k_BT)}{\int \exp(-V'(\chi)/k_BT)\, d\chi} \quad (27)$$

with

$$V'(\chi) = \text{const} - k_BT \ln Q_{\Omega,Z}(\chi) \quad (28)$$

If the constant is taken such that $V'(\chi) = V(\chi)$ for $U(\Omega,Z,\chi) = 0$, eq 28 defines an effective torsional potential in the water/bilayer environment. Given the nonuniform character of this system, a more meaningful property should retain the position dependence. A depth-dependent effective torsional potential $V'(Z,\chi)$ can be defined, from the reduced distribution function:

$$P_\Omega(Z, \chi) = \frac{Q_\Omega(Z, \chi)}{Q} \quad (29)$$

with

$$Q_\Omega(Z, \chi) = \exp(-V(\chi)/k_BT) \int \exp(-U(\Omega, Z, \chi)/k_BT)\, d\Omega \quad (30)$$

and the normalization condition $\int_0^L dZ \int P_\Omega(Z,\chi)\, d\chi = 1$. The effective torsional potential is then defined as

$$V'(Z, \chi) = c(Z) - k_BT \ln Q_\Omega(Z, \chi) \quad (31)$$

with $c(Z)$ chosen in such a way that $V'(Z,\chi) = V(\chi)$ for $U(\Omega,Z,\chi) = 0$.

The average value $\langle f \rangle$ of any arbitrary function $f(\Omega,Z,\chi)$ can be calculated as

$$\langle f \rangle = \int_0^L dZ \int d\Omega \int f(\Omega, Z, \chi)\, P(\Omega, Z, \chi)\, d\chi \quad (32)$$

The partially averaged function can also be defined, in analogy with eq 19. In particular, the positional-orientational average for a given conformation can be calculated as

$$\langle f \rangle_{\Omega,Z}(\chi) = \frac{1}{P_{\Omega,Z}(\chi)} \int_0^L dZ \int f(\Omega, Z)\, P(\Omega, Z, \chi)\, d\Omega \quad (33)$$

This is the property that would be calculated for the molecule frozen in the conformation specified by the χ dihedrals. The full average, eq 32 can be obtained from partial averages, eq 33, as $\langle f \rangle = \int \langle f \rangle_{\Omega,Z}(\chi)\, P_{\Omega,Z}(\chi)\, d\chi$.

If the torsional potential is characterized by localized minima, separated by barriers higher than few k_BT units, the molecular flexibility can be described in terms of a finite number of conformers, corresponding to minima of the potential energy.[48] Then, the single conformer orientational-positional distribution function

$$P_J(\Omega, Z) = \frac{\exp(-V_J/k_BT)\exp(-U_J(\Omega, Z)/k_BT)}{Q} \quad (34)$$

can be introduced, where the index J is used to indicate functions calculated for the Jth conformer ($\chi = \chi_J$), and integration over the χ dihedrals can be replaced by summation over conformers; for instance,

$$Q = \sum_J \int_0^L dZ \int \exp(-V_J/k_BT)\exp(-U_J(\Omega, Z)/k_BT)\, d\Omega$$

Numerical Methods

Computation of each of the contributions to the mean field potential, eq 1, requires a definition of the solute molecular surface. The solvent-excluded surface,[49] calculated as a triangulated surface according to the Sanner algorithm,[50] is used. The expressions used to calculate eqs 2, 5, 6, and 11 are reported in the following. In these expressions N_f represents the number of triangular faces, $\mathbf{s}_J$, with components $s_{J,X}$, $s_{J,Y}$, and $s_{J,Z}$ in the bilayer frame, is the outward pointing unit vector normal to the Jth face, and S_J is the surface area of this face.

The volume integral in eq 2 is calculated as the sum over N_s slices of thickness $\Delta z'$ perpendicular to the bilayer normal:

$$\int_{\substack{\text{molecular}\\ \text{length}}} \pi(Z+z')\,\sigma(\Omega, Z+z')\,\mathrm{d}z' = \sum_{i=1}^{N_s} \pi(Z+z'_i)\,\sigma(\Omega, Z+z'_i)\,\Delta z' \quad (35)$$

The section area, $\sigma(\Omega,Z + z'_i)$, is calculated from the perimeter of the λ-sided polygon, defined by the intersection of the triangulated surface with the ith plane, according to Surveyor's formula for non self-intersecting polygons:[51]

$$\sigma(Z+z'_i) = \left|\frac{1}{2}\sum_{\alpha=1}^{\lambda}(x'_\alpha y'_{\alpha+1} - x'_{\alpha+1}y'_\alpha)\right| \quad (36)$$

where (x'_α,y'_α), with $\alpha = 1-\lambda$, are the coordinates of the polygon vertices, ordered according to consecutive sides, with the boundary condition $(x'_{\lambda+1},y'_{\lambda+1}) = (x'_1,y'_1)$.

The volume integrals A_{ni}, defined in eq 5, are conveniently rewritten in the form of surface integrals, using Gauss's theorem:[52]

$$A_{ni} = \left[\frac{1}{n-3}\left(\frac{1}{(R_i^{\mathrm{vdW}})^{n-3}} - \frac{1}{4\pi}\int_{\substack{\text{molecular}\\ \text{volume}\\ r>R_i^{\mathrm{vdW}}}}\left(-\nabla\cdot\frac{\mathbf{r}}{r^n}\right)\mathrm{d}\mathbf{r}\right)\right]^{1/(n-3)} = \left[\frac{1}{4(n-3)\pi}\int_S \frac{\mathbf{r}}{r^n}\cdot\mathbf{s}\,\mathrm{d}S\right]^{1/(n-3)} \quad (37)$$

The integral is then calculated as a sum over the triangular faces:

$$A_{ni} = \left(\frac{1}{4(n-3)\pi}\sum_{J=1}^{N_f}\frac{\mathbf{r}_{iJ}}{r_{iJ}^n}\cdot\mathbf{s}_J S_J\right)^{1/(n-3)} \quad (38)$$

where $\mathbf{r}_{iJ}$ is the vector from the center of the ith atom to the center of mass of the Jth face.

Due to the axial symmetry of the bilayer, the volume integral in eq 6 is conveniently calculated in cylindrical coordinates (z',q,ϕ):

$$\begin{aligned}\int_{\substack{\text{solvent}\\ r>R_{ij}}}\frac{\rho_j(Z_i+z')}{r'^6}\,\mathrm{d}\mathbf{r}' &= \int_{R_{ij}}^{z'_{\max}}\rho_j(Z_i+z')\,\mathrm{d}z'\int_0^\infty\frac{q}{(q^2+z'^2)^3}\,\mathrm{d}q\int_0^{2\pi}\mathrm{d}\phi\\ &+ \int_{-R_{ij}}^{R_{ij}}\rho_j(Z_i+z')\,\mathrm{d}z'\int_{\sqrt{R_{ij}^2-z'^2}}^\infty\frac{q}{(q^2+z'^2)^3}\,\mathrm{d}q\int_0^{2\pi}\mathrm{d}\phi\\ &+ \int_{-z'_{\max}}^{-R_{ij}}\rho_j(Z_i+z')\,\mathrm{d}z'\int_0^\infty\frac{q}{(q^2+z'^2)^3}\,\mathrm{d}q\int_0^{2\pi}\mathrm{d}\phi\\ &= \frac{\pi}{2}\left[\int_{R_{ij}}^{z'_{\max}}\frac{\rho_j(Z_i+z')}{z'^4}\,\mathrm{d}z' + \frac{1}{R_{ij}^4}\int_{-R_{ij}}^{R_{ij}}\rho_j(Z_i+z')\,\mathrm{d}z' + \int_{-z'_{\max}}^{-R_{ij}}\frac{\rho_j(Z_i+z')}{z'^4}\,\mathrm{d}z'\right]\end{aligned} \quad (39)$$

where $R_{ij} = R_i^d + R_j^{\mathrm{vdW}}$. Under the assumption that the size of the sample is much larger than R_{ij}, the integrals over the q variable are calculated by extending to infinity the upper integration limit. In our calculations, $z'_{\max} = 4R_{ij}$ was taken. The three integrals in the final expression are calculated with the composite midpoint formula.[53]

The surface integral in eq 11 is simply calculated as the sum over all triangular faces:

$$\int_S \xi(Z+z')\,P_2(\cos\theta)\,\mathrm{d}S = \sum_{J=1}^{N_f}\xi(Z+z'_J)\frac{3s_{J,Z}^2-1}{2}S_J \quad (40)$$

where the position of the Jth face is identified with that of its center of mass.

Free Energy Profiles and Average Quantities. Gauss−Legendre and Gauss−Chebyshev quadrature algorithms were used for numerical integration over the orientational variables β and γ, respectively.[53] Numerical integration over the position variable Z was simply performed according to the composite midpoint formula; calculations for cholesterol in DPPC were performed giving the upper integration limit the value L = 45 Å. Convergence of numerical integrals was checked for free energy profiles and other average properties. A typical calculation, using 12 β, 24 γ, and 91 Z points, takes on the order of hundreds of seconds of CPU time on a 2 GHz desktop PC.

Cholesterol in DPPC

Bilayer Parametrization. Figure 2 shows the profiles of bilayer properties needed for the calculations. Lateral pressure,[54] mass density,[55] and S_{CD} order parameter[56] profiles were taken from molecular dynamics simulations of a DPPC bilayer in the liquid crystal phase at the temperature T = 323 K. The definition of polarizable units and the corresponding mass density profiles, appearing in eq 6, are reported in Figure S2 (Supporting Information); the value $I = 2\times10^{-18}$ J[57] was assumed in this equation. The outer dielectric constant profiles, used in eqs 3 and 4, were calculated on the basis of a three-dielectric model, as proposed in ref 14. The empirical parameters appearing in eq 4 were determined by matching electrostatic free energies, calculated according to eq 3, to those calculated by the finite difference solution of the Poisson equation, for a test set of molecules (see SI-3, Supporting Information). Parts of the same molecules were used to check calculated water/*n*-octanol transfer free energies against experimental values (see SI-4, Supporting Information). Given the S_{CD} order parameters, the profile of the orienting strength, $\xi(Z)$, entering eq 11, was obtained by nonlinear fitting of the values calculated at the average acyl chain carbon positions, $\xi(\langle Z_i\rangle)$ (see SI-1, Supporting Information).

Solute Structural Data. Nine conformers of cholesterol differing in the alkyl chain conformation were taken for our calculations (see Figure S6, Supporting Information). Conformer energy and geometry were obtained by DFT optimization in a vacuum at the B3LYP/6-31g** level.[58] A common molecular frame was chosen for all conformers, with the origin at the nuclear position of the oxygen atom

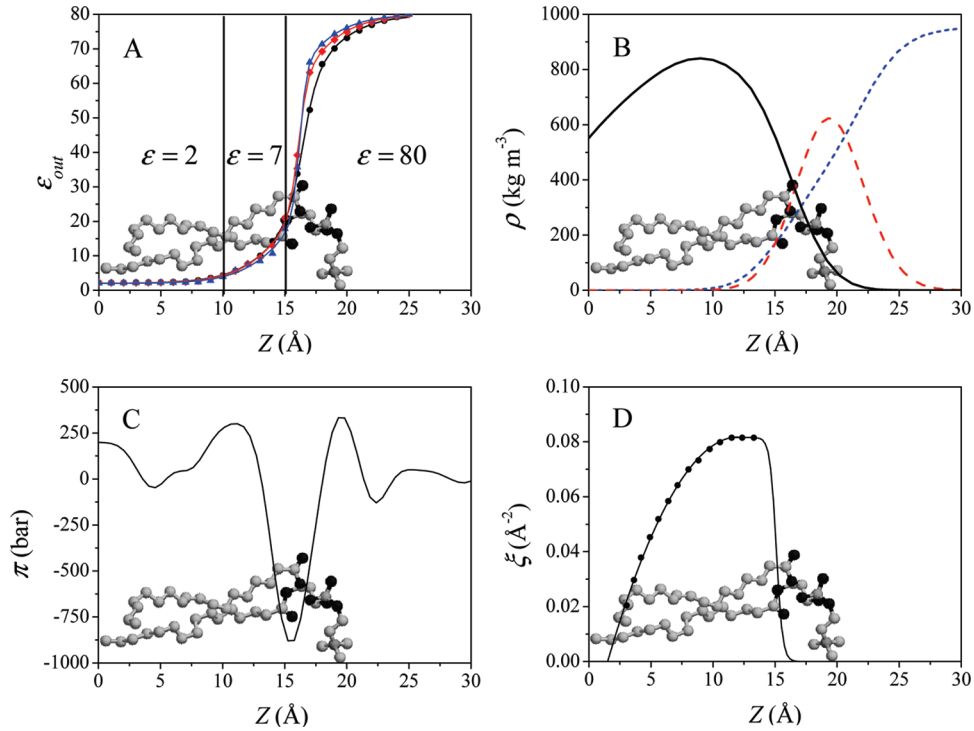

Figure 2. DPPC properties used in the calculations, shown as a function of the distance from bilayer midplane. (A) Local dielectric constant profile calculated with a three-dielectric model, as described in ref 14, for ions of van der Waals radius equal to 1 Å (triangles), 1.85 Å (circles), and 1.5 Å (squares). (B) Mass density profile for lipid tails (solid line), lipid headgroups (dashed line), and water (dotted line).[55] (C) Lateral pressure profile.[54] (D) Orienting strength profile from S_{CD} order parameters for the *sn*1 acyl chain.[56] All of the data refer to the temperature $T = 323$ K. A phospholipid molecules is superimposed on each plot, to indicate different bilayer regions.

Table 1. Parameters Used in Calculations for Cholesterol

van der Waals radii	H, 1.00 Å; C, 1.85 Å; O, 1.50 Å[59]
Connolly surface	probe sphere radius =3 Å; vertex density =13 Å^{-2}
atomic charges	OPLS force field[60] (see Table S1, Supporting Information)
atomic polarizabilities ($4\pi\varepsilon_0$ Å^3)	from bond polarizabilities[57] [a] H−C: 0.65; C−C: 0.57; C=C: 1.65; C−O: 0.64; O−H: 0.73
internal dielectric constant	$\varepsilon_{in} = 2$[14]
Born empirical parameters	$F = 8$; $C_0 = 0.3028$; $C_1 = 1.009$; $D = 0.00$ Å^{-1}; $E = -0.16$ Å^{-1} [b]

[a] Half of a bond polarizability is assigned to each of the two connected atoms; hence the polarizability of an atom is obtained as half the sum of the polarizabilities of all the bonds in which it is involved. [b] Obtained from optimization with respect to the finite difference solution of the Poisson equation, for a test set of benzene derivatives (see SI-3, Supporting Information), according to the procedure reported in ref 61.

and the (x,y,z) axes fixed to the rigid core, as shown in Figure 1. Solute parameters used for calculations are summarized in Table 1.

Results

Free Energy and Distributions. Figure 3 displays the transfer free energy profile and the corresponding position distribution function, calculated by averaging over all nine conformers of cholesterol. The transfer free energy profile exhibits a marked position dependence, not only near the water/bilayer interface but also in the hydrocarbon region. The free energy minimum, which is about 13 kcal/mol lower than the free energy in bulk water, is reached when cholesterol is inserted in the bilayer, with the oxygen at a distance of about 18 Å from the midplane. The position distribution function $P_{\Omega\chi}$, shown in Figure 3, indicates that cholesterol, though confined with the oxygen atom near the hydrophobic/hydrophilic interface, may undergo wide-amplitude fluctuations parallel to the bilayer normal. Both the average position and the vertical distribution of cholesterol are in agreement with experimental data. By recent neutron scattering experiments, the center of mass of deuteriated sites of [2,2,3,4,4,6-$^2H_6$]-labeled cholesterol, in the liquid crystalline phase of different lipid bilayers, was found to be confined in a region a few Ångstroms wide, centered at approximately 16 Å from the midplane.[62] Vertical motions of cholesterol wider than 5 Å were also revealed by quasielastic neutron scattering experiments in 40% cholesterol:DPPC bilayers in the liquid ordered phase.[63]

The tail flexibility has negligible effects on the free energy profile of cholesterol (see Figure S7, Supporting Information), which is not surprising, given the small size of the alkyl chain in comparison to the broad ring region and the reduced conformational space explored by the tail, due to steric constraints. For this reason in the following, until differently stated, we will simply refer to the results obtained

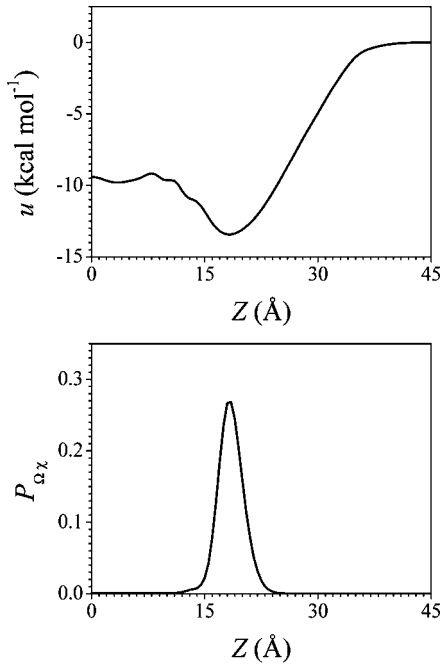

Figure 3. Transfer free energy (top) and position distribution (bottom) profiles of cholesterol as a function of distance of the oxygen atom from the bilayer midplane. The results shown here were obtained as averages over all conformers at the temperature $T = 323$ K.

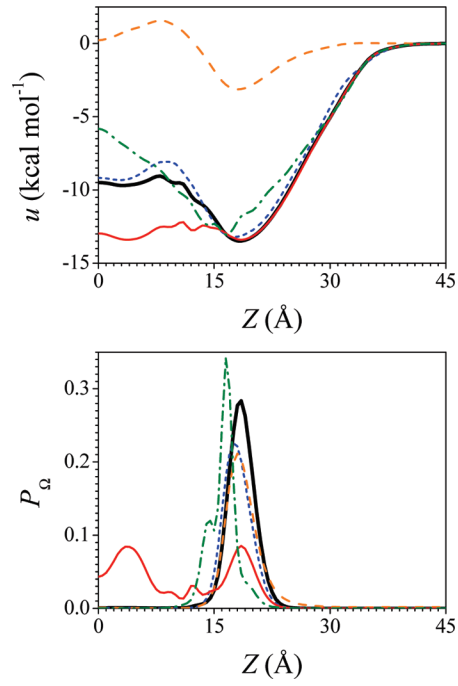

Figure 4. Transfer free energy (top) and position distribution (bottom) profiles calculated for cholesterol as a function of the distance of the oxygen atom from the bilayer midplane, using an incomplete form of the mean field potential $U(\Omega,Z)$. Profiles were obtained by excluding in turn the single cavity (thin dotted line), the electrostatic (thin solid line), the dispersion (thin dashed line), and the chain order (thin dash-dotted line) contributions in eq 1. The profiles from the complete form of the potential (thick solid line) are also shown for comparison. The results shown here were obtained for the B conformer, at the temperature $T = 323$ K.

for the B conformer of cholesterol (see Figure S6, Supporting Information).

With the purpose of disentangling the role of the different contributions to the mean field potential, we show in Figure 4 the free energy profiles and the corresponding position distribution functions, obtained by excluding a single contribution at a time in eq 1. The figure clearly shows that dispersion interactions bear the main responsibility for the free energy decrease within the bilayer, in agreement with the simple picture of cholesterol brought into the bilayer by favorable interactions with lipid chains. Electrostatic interactions, which in the case of cholesterol mostly involve the OH group, have the effect of destabilizing upside-down configurations, with this group located deep in the bilayer interior. The effects of the order and cavity contribution to the mean field potential will be clearer below, when the order parameters of cholesterol are discussed; however, something can be anticipated in relation to the transfer free energy and the distribution profiles shown in Figure 4. The order contribution promotes alignment of the long axis of cholesterol to the director, i.e., the average orientation of acyl chains, which in the liquid crystalline phase of DPPC coincides with the bilayer normal **N**. The small shift of the oxygen atom toward the lipid headgroups, which we can observe in Figure 4 upon inclusion of the order contribution in the mean field potential, can be explained by the fact that it allows a larger portion of the broad and thick core of cholesterol to lie in the most ordered lipid region (it may be useful to look at the molecular surface of cholesterol, which is shown in Figure S8, Supporting Information). Given the strong orienting effect of the ordering term, the cavity contribution, which would bring about the insertion of cholesterol flat at the hydrophobic/hydrophilic interface, where there is a deep well in the lateral pressure, seems to play a minor role.

The free energy profile shown in Figure 3 compares well with that reported in Figure 1b of ref 64, which was obtained from long all-atom molecular dynamics simulations (3-μs-long trajectories) of cholesterol in DPPC. Perhaps more interestingly, the relatively small differences between the free energy profiles obtained from all-atom simulations of cholesterol and its analog missing the hydroxyl group in DPPC, displayed in Figure S5 of the same reference,[64] closely resemble the differences arising from removing electrostatic interactions in our model, as shown in Figure 4. There is however a scale factor: the transfer free energy calculated with our model is about 30% lower, in absolute value, than that obtained from simulations, which probably reflects a different parametrization of interactions. In fact, discrepancies of this magnitude are not uncommon even between simulations using different force fields.

A major feature of our model is the inclusion of orientation−position coupling inside the lipid bilayer. Figure 5 shows the map of the mean field potential, calculated in correspondence of the maximum of the position distribution probability, as a function of the Euler angles (β,γ), defining the molecular orientation. The figure shows a strong dependence of the potential on the Euler angle β between the long

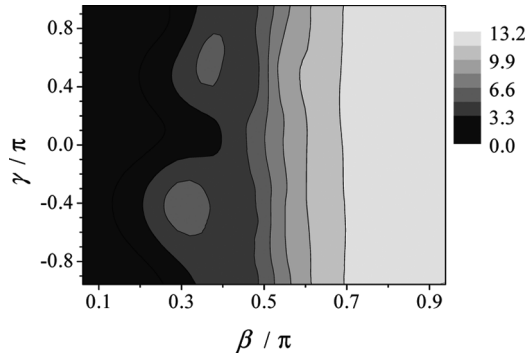

Figure 5. Contour plot of the mean field potential *U*, eq 1, as a function of the Euler angles (β,γ) defining the solute orientation in the bilayer frame (Figure 1), calculated in correspondence of the maximum of the position distribution. The results shown here were obtained for the B conformer of cholesterol at the temperature $T = 323$ K. Energies are expressed in kcal mol^{-1}, and a value equal to zero is given to the minimum of the mean field potential in the plot.

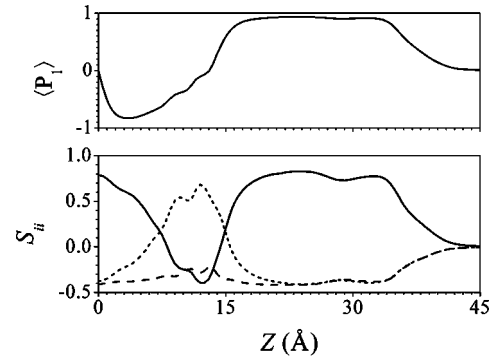

Figure 6. Local orientational order parameters calculated for cholesterol as a function of the distance of the oxygen atom from the bilayer midplane. The plot at the bottom shows the diagonal elements of the Saupe tensor, calculated in the molecular frame (Figure 1): S_{xx} (dotted line), S_{yy} (dashed line), and S_{zz} (solid line). The results shown here were obtained for the B conformer, at the temperature $T = 323$ K.

axis of cholesterol and the bilayer normal (see Figure 1), with the energy increasing as cholesterol moves from parallel to antiparallel. The dependence of the mean field potential on the γ angle indicates that cholesterol has some preference to keep the molecular plane (i.e., the *xz* plane) parallel to the bilayer normal.

A complete insight into the orientational behavior of the solute is provided by orientational order parameters. The order parameter $\langle P_1 \rangle = \langle \cos \beta \rangle$ describes the polarity of the orientational distribution; it can take values ranging from -1 to $+1$, with the extremes corresponding to the molecular *z* axis antiparallel and parallel to the bilayer normal, respectively, going through 0 for an apolar distribution. The second rank order parameters $S_{ii} = (3\langle \cos^2 \theta_{iZ} \rangle - 1)/2$, with θ_{iZ} denoting the angle between the *i*th molecular axis ($i = x,y,z$) and the bilayer normal, quantify the degree of alignment of molecular axes to the bilayer normal. Unlike $\langle P_1 \rangle$, the S_{ii} order parameters do not distinguish between parallel and antiparallel orientations; they range between -0.5 (*i* axis perpendicular to the director) and $+1$ (*i* axis parallel to the director). Figure 6 shows the profile of the order parameters $\langle P_1 \rangle$ and S_{ii} calculated for the B conformer of cholesterol. Here, we can distinguish at least three zones: (i) a first region where cholesterol is in upright orientations, well aligned to the bilayer normal **N** with its head in water or in the hydrophilic region, pointing toward water; (ii) a second region where the oxygen atom is close to the midplane and the long axis is again aligned to **N**; (iii) an intermediate region, where cholesterol lies inside the bilayer, with its long axis preferentially perpendicular to **N** and the molecular plane perpendicular to the bilayer plane. The result is a clear indication of the peculiar effects of the nanoscale organization of lipid bilayers. It must be remarked that the probability that cholesterol resides in the ii or in the iii regions is negligible, as shown in Figure 3. This is in agreement with the absence of experimental evidence for cholesterol lying flat inside DPPC bilayers. However, we can speculate that such orientations may be favored under different conditions, e.g., when the nature of phospholipids leads to a different balance of forces within the bilayer. Indeed, the existence of the horizontal orientation of cholesterol in polyunsaturated phospholipids was recently demonstrated by neutron scattering investigations.[62,65] Some preference for orientations parallel to the bilayer plane was also found in atomistic simulations of cholesterol, sitting in scarcely populated regions inside DPPC or other lipid bilayers.[64]

With the help of Figure 7, which shows the order parameters calculated by excluding one contribution at a time, we can now distinguish the different contributions to the orientational order of cholesterol. From inspection of the plots in this figure, we can draw the following picture. The anisotropy of interactions of cholesterol with acyl chains bears the main, although not the only, responsibility for the orientational order of cholesterol across the bilayer. In its absence (Figure 7D), cholesterol would be significantly ordered in two zones, by virtue of dispersion and the cavity contributions. In the former region, part of cholesterol, comprising the oxygen atom, lies in water, and alignment of the long axis to the normal allows the molecule to insert as much as possible of its body into the bilayer. In the latter region, the drop in lateral pressure at approximately 15 Å from the midplane and the optimization of the dispersion interaction when a large portion of the solute resides in the region around 10 Å promote horizontal orientation of the long molecular axis. Inclusion of the anisotropic interactions with acyl chains increases the degree of alignment of the long axis of cholesterol, when this is parallel to the bilayer normal, and differently stabilizes the orientations of the molecular plane, when the long axis lies perpendicular to the normal: orientations with this plane parallel are favored over those with the plane perpendicular to lipid chains. Electrostatic interactions, which have the main responsibility for keeping the polar group of cholesterol in the hydrophilic region, are not very important for the orientational order of this molecule.

Accurate information on orientational order is obtained from quadrupole splittings in NMR spectra of specifically deuteriated samples. We have calculated the order parameters

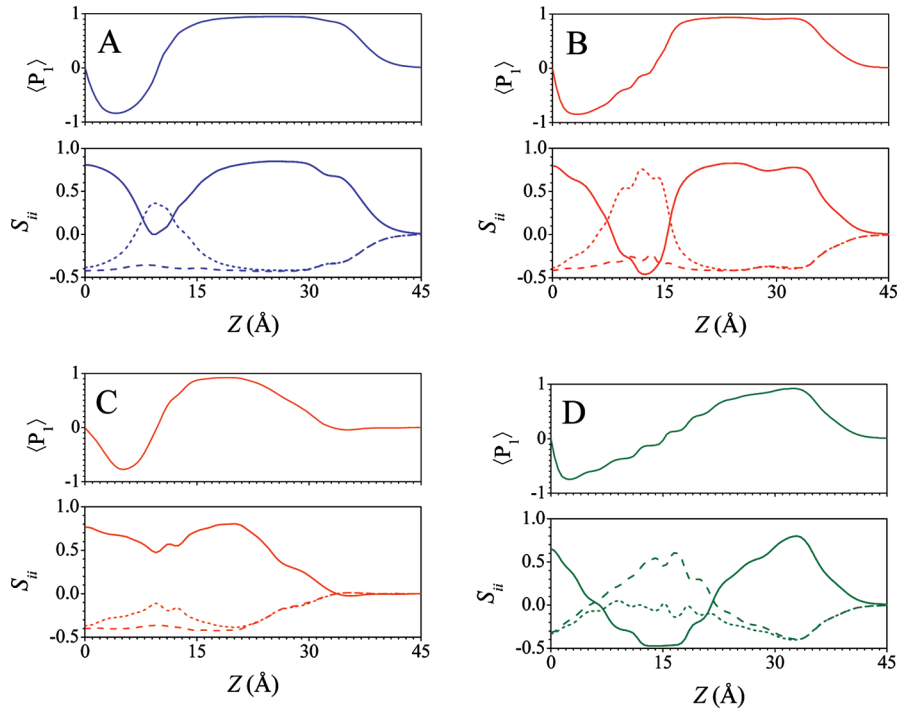

Figure 7. Local orientational order parameters calculated for cholesterol as a function of the distance of the oxygen atom from the bilayer midplane, using an incomplete form of the potential $U(\Omega,Z)$ in eq 1 of the main text. The results shown here were obtained by excluding in turn the cavity (A), the electrostatic (B), the dispersion (C), and the chain order (D) contributions in eq 1. For each case, the plot at the top displays the orientational average of the first Legendre polynomial, $\langle P_1 \rangle$, whereas that at the bottom shows the diagonal elements of the Saupe tensor, calculated in the molecular frame (Figure 1): S_{xx} (dotted line), S_{yy} (dashed line), and S_{zz} (solid line). The results shown here were obtained for the B conformer at the temperature $T = 323$ K.

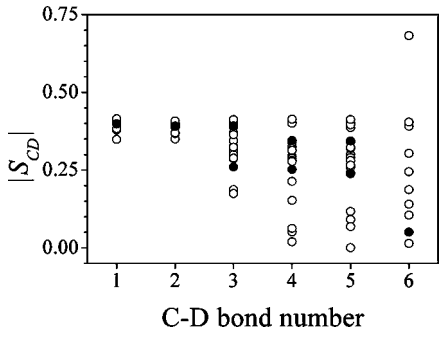

Figure 8. $|S_{CD}|$ order parameters, calculated for the alkyl chain of cholesterol at the temperature $T = 323$ K. Full symbols: averages over conformers. Open symbols: individual conformers. Bonds are numbered as follows: 1 for C_{17}−D, 2 for C_{20}−D, 3 for C_{22}−D, 4 for C_{23}−D, 5 for C_{24}−D, and 6 for C_{25}−D (atom numbering as in Figure S5, Supporting Information).

for the C_3H bond and the tail CH bonds (see Figure S5, Supporting Information), defined as in eq 8, which can be directly compared with experimental data. The value $S_{CD} = -0.33$ was obtained for the C_3H bond after averaging over all nine conformers; the negative sign indicates the tendency of this bond to lie perpendicular to the bilayer normal. Figure 8 shows the position dependence of the $|S_{CD}|$ order parameters calculated for the alkyl chain CH bonds of cholesterol. In addition to the order parameters obtained as averages over all nine conformers, those calculated for the single conformers are shown; the former and the latter would correspond to experimental data for fast and slow conformational motions (on the NMR time scale), respectively. We can see that, for bonds between C_{22} and C_{24}, significantly different order parameters are predicted for the nine conformers, due to their different chain geometry. We can also see that, even after the conformational average, different order parameters are obtained for the pairs of deuterons at C_{22}, C_{23}, and C_{24}; this means that deuterons linked to the same carbon atom have a different average orientation in the bilayer. Quadrupole spectra of cholesterol specifically deuterated at C_{24} were reported for a wide range of temperatures in the liquid crystal phase of 3:7 (molar ratio) cholesterol/DMPC mixtures.[67] From the quadrupole splittings, 33.2 and 42 kHz, measured at about 10 °C above the melting temperature, $|S_{CD}|$ values equal to 0.26 and 0.33, respectively, can be estimated, assuming a deuterium quadrupole coupling constant equal to 170 kHz.[68] The average order parameters calculated for the two C_{24}−D bonds, S_{CD}=−0.24 and $S_{CD} = -0.34$, are in line with experimental results. As for the C_3H bond, the quadrupole splitting $\Delta\nu \sim 84$ kHz was reported in ref 66 for 5 mol % cholesterol in DPPC at the temperature $T = 47$ °C, from which the value $|S_{CD}| \sim 0.33$ is derived, assuming again a deuterium quadrupole coupling constant equal to 170 kHz. The agreement between predicted and experimental order parameters for different sites is a good check for the ability of our model to predict the orientational behavior of cholesterol in the bilayer environment.

Finally, we report in Table 2 a list of properties calculated for cholesterol by averaging over all degrees of freedom (translational, orientational and conformational), according to eq 32. Such averages make sense in the case of cholesterol,

Table 2. Average Properties Calculated for Cholesterol in DPPC Bilayer at the Temperature $T = 323$ K[a]

$\langle Z \rangle$	$\langle P_1 \rangle$	S_{xx}	S_{yy}	S_{zz}
18.5 Å	0.86	−0.31	−0.45	0.76

[a] $\langle Z \rangle$ is the average distance of the oxygen atom from the midplane. $\langle P_1 \rangle$ is the average value of the cosine of the angle between the bilayer normal and the z molecular axis (Figure 1), and S_{ii} ($i = x,y,z$) are the principal values of the Saupe matrix.

which is predicted to be mostly confined in a region with uniform orientational behavior within the bilayer. The properties reported in Table 2 are close to those calculated for the single A or B conformers (see Figure S6, Supporting Information); these are very similar to each other and are predicted to be significantly more probable than the other conformers. In fact, not only A and B are, according to DFT calculations, the most stable in a vacuum, but they are further stabilized by the bilayer environment, as shown by the values of the difference $\Delta V_J = V'_J - V_J$, calculated according to eq 28 and reported in Figure S6. The very high $\langle P_1 \rangle$ value, close to 1, indicates the strong preference of cholesterol for orientations parallel to the bilayer normal with the hydroxyl group pointing toward water, over antiparallel orientations. The preference for parallel over perpendicular orientation of the long molecular axis is quantified by the $S_{z'z'}$ value. The principal axis system of the Saupe matrix (x',y',z'), shown in Figure S9 (Supporting Information), does not exactly coincide with the molecular frame (x,y,z); in particular, the major alignment axis (z') is tilted by about 14° with respect to the molecular z axis (shown in Figure 1). Of the two other principal alignment axes, y', nearly perpendicular to the molecular plane, is predicted to have a higher tendency to lie perpendicular to the bilayer normal than x'.

Conclusions

In a recent review, the need of new implicit models of membranes, combining an atomistic solute representation with a better account of the bilayer structure, was stressed.[2] The present work is an effort in this direction; the main new features, which are generally ignored by the existing models, are summarized as follows.

The anisotropy and nonuniformity of the bilayer environment are included, in a way that allows for a realistic account of the chemical composition and physical state of the phospholipid system; they are introduced through the profiles of lateral pressure, density, order parameters and dielectric permittivity. Appropriate values of these for a given membrane can be derived from experiments or from atomistic simulations. The elastic response of the bilayer is, at least in part, implicitly contained in the cavity contribution to the mean field potential.

The full solute distribution function, accounting for the coupling between molecular position, orientation, and conformation, is calculated. Detailed information is provided, not only on the preferred configurations but also on fluctuations about them. This is important to get a realistic description of the behavior in the fluid bilayer environment where solutes, though confined, may undergo wide displacements and reorientations, which are likely to be essential for their biophysical role.

In its present form, the model ignores the membrane perturbation induced by the solute; therefore it is not suitable at high solute concentrations. However, the theoretical framework presented here allows the inclusion of the bilayer response, and future effort in this direction is planned.

To illustrate the capability of our model, we have presented the case study of cholesterol in DPPC. We have calculated a variety of properties, showing that the method proposed here is suitable for a general description of solutes in the bilayer environment. The use of the model allows us to disentangle the different contributions to solute properties in the bilayer and to shed light on the often unexpected effects of the anisotropy and nonuniformity of this environment. Small conformational effects are found for cholesterol, which is not surprising, in view of the small size of the flexible tail, if compared with the broad rigid core. Comparison of our results with experiments and simulations is very encouraging. The free energy profile calculated for cholesterol across the bilayer exhibits the same features as the profile obtained from all-atom molecular dynamics simulations.[63] Strong position/orientation couplings emerge: cholesterol is predicted to be mostly buried in the bilayer, with its head in the hydrophilic region and its long axis nearly perpendicular to the surface. When embedded deeper in the bilayer, cholesterol is predicted to change its average orientation and to preferentially keep its long axis parallel to the surface. According to our calculations, the latter configurations should have a very low probability for cholesterol in liquid crystalline DPPC; however, they may become more significant in other lipid systems. Interestingly, cholesterol lying flat, close to the bilayer center, was recently revealed by neutron scattering studies in unsaturated lipids.[64,65]

The method proposed here is computationally cheap. A detailed insight into the properties of a given solute/bilayer pair can be reached at very low cost, so we think that it could be usefully exploited for different purposes. It can provide the free energy landscapes needed to model solute permeability through membranes. Moreover, it may be suitable to mimic the bilayer environment in Monte Carlo and molecular dynamics simulations and to be integrated with quantum mechanical calculations of spectroscopic observables in lipid membranes.[69]

Abbreviations

DPPC, 1,2-dipalmitoyl-*sn*-glycero-3-phosphatidylcholine; DMPC, 1,2-dimyristoyl-*sn*-glycero-3-phosphatidylcholine; DFT, density functional theory.

Acknowledgment. This work was supported by the University of Padova (ex 60%). We are grateful to Dr. Matteo Stocchero for stimulating discussions and insightful comments during the course of this work. We gratefully acknowledge an anonymous reviewer for valuable criticism and suggestions.

Supporting Information Available: Derivation of the relationship between orienting strength ξ and S_{CD} order

parameters; definition of polarizable units in DPPC and corresponding mass density profiles; list of molecules used to parametrize the electrostatic contribution to the mean field potential; calculated and experimental water/*n*-octanol transfer free energies; atom labels and OPLS charges for cholesterol; list of cholesterol conformers considered in calculations with their torsional energy; representation of the molecular surface of cholesterol and of the principal axis system of its Saupe ordering tensor; plot of transfer free energy calculated for nine conformers of cholesterol in DPPC. This information is available free of charge via the Internet at http://pubs.acs.org/.

References

(1) White, S. H.; Wimpley, W. C. Membrane protein folding and stability: physical principles. *Annu. Rev. Biophys. Biomol. Struct.* **1999**, *28*, 319–365.

(2) Grossfield, A. Implicit modeling of membranes. *Curr. Topics Membr.* **2008**, *60*, 131–157.

(3) De Young, L. R.; Dill, K. A. Solute partitioning into lipid bilayer membranes. *Biochemistry* **1988**, *27*, 5281–5289.

(4) Marqusee, J. A.; Dill, K. A. Solute partitioning into chain molecule interphases: monolayers, bilayer membranes, and micelles. *J. Chem. Phys.* **1986**, *85*, 434–444.

(5) Tobias, D. J. Electrostatic calculations: recent methodological advances and applications to membranes. *Curr. Opin. Struct. Biol.* **2001**, *11*, 253–261.

(6) Feig, M.; Brooks, C. L. Recent advances in the development and application of implicit solvent models in biomolecule simulations. *Curr. Opin. Struct. Biol.* **2004**, *14*, 217–224.

(7) Chen, J.; Brooks, C. L.; Khandogin, J. Recent advances in implicit solvent-based methods for biomolecular simulations. *Curr. Opin. Struct. Biol.* **2008**, *18*, 140–148.

(8) Fattal, D. R.; Ben-Shaul, A. A molecular model for lipid-protein interactions in membranes: the role of hydrophobic mismatch. *Biophys. J.* **1993**, *65*, 1795–1809.

(9) Fattal, D. R.; Ben-Shaul, A. Mean-field calculations of chain packing and conformational statistics in lipid bilayers: comparison with experiments and molecular dynamics studies. *Biophys. J.* **1994**, *67*, 983–995.

(10) Xiang, T.; Anderson, B. Molecular distributions in interphases: statistical mechanical theory combined with Molecular Dynamics simulation of a model lipid bilayer. *Biophys. J.* **1994**, *66*, 561–572.

(11) Mitragotri, S.; Johnson, M. E.; Blankschtein, D.; Langer, R. An analysis of the size selectivity of solute partitioning, diffusion, and permeation across lipid bilayers. *Biophys. J.* **1999**, *77*, 1268–1283.

(12) Kessel, A.; Ben-Tal, N.; May, S. Interactions of cholesterol with lipid bilayers: the preferred configuration and fluctuations. *Biophys. J.* **2001**, *81*, 643–658.

(13) Cantor, R. S. Lateral pressures in cell membranes: a mechanism for modulation of protein function. *J. Phys. Chem.* **1997**, *101*, 1723–1725.

(14) Tanizaki, S.; Feig, M. A generalized Born formalism for heterogeneous dielectric environments: application to the implicit modeling of biological membranes. *J. Chem. Phys.* **2005**, *122*, 124706:1–13.

(15) Ferrarini, A.; Moro, G. J.; Nordio, P. L.; Luckhurst, G. R. A shape model for molecular ordering in nematics. *Mol. Phys.* **1992**, *77*, 1–15.

(16) Mennucci, B.; Cammi, R. *Continuum Solvation Models in Chemical Physics*; Wiley: Chichester, U. K., 2007.

(17) Cantor, R. S. Lipid composition and the lateral pressure profile in bilayers. *Biophys. J.* **1999**, *76*, 2625–2639.

(18) Cantor, R. S. The influence of membrane lateral pressures on simple geometric models of protein conformational equilibria. *Chem. Phys. Lipids* **1999**, *101*, 45–56.

(19) Marsh, D. Lateral pressure in membranes. *Biochim. Biophys. Acta* **1996**, *1286*, 183–223.

(20) Patra, M. Lateral pressure profiles in cholesterol-DPPC bilayers. *Eur. Biophys. J.* **2005**, *35*, 79–88.

(21) Baoukina, S.; Marrink, S. J.; Tieleman, D. P. Lateral pressure profiles in lipid monolayers. *Faraday Disc.* **2010**, *144*, 393–409.

(22) Rowlinson, J. S.; Widom, B. *Molecular Theory of Capillarity*; Clarendon: Oxford, U. K., 1982.

(23) Helfrich, W. In *Physics of Defects*; Balian, R., Kleman, M., Poirier, J. P., Eds.; North-Holland Publishing: Amsterdam, 1981; pp 716−755.

(24) Szleifer, I.; Kramer, D.; Ben-Shaul, A.; Gelbart, W. M.; Safran, S. A. Molecular theory of curvature elasticity in surfactant films. *J. Chem. Phys.* **1990**, *92*, 6800–6817.

(25) Kozlov, M. M. In *Soft Condensed Matter Physics in Molecular and Cell Biology*; Poon, W. C. H., Andelman, D., Eds.; Taylor & Francis: Boca Raton, FL, 2006; pp 79−96.

(26) Honig, B.; Sharp, K.; Yang, A.-S. Macroscopic models of aqueous solutions: biological and chemical applications. *J. Phys. Chem.* **1993**, *97*, 1101–1109.

(27) Baker, N. A. Poisson-Boltzmann methods for biomolecular electrostatics. *Methods Enzymol.* **2004**, *383*, 94–118.

(28) Still, W. C.; Tempczyk, A.; Hawley, R. C.; Hendrickson, T. Semianalytical treatment of solvation for molecular mechanics and dynamics. *J. Am. Chem. Soc.* **1990**, *112*, 6127–6129.

(29) Bashford, D.; Case, D. A. Generalized Born models of macromolecular solvation effects. *Annu. Rev. Phys. Chem.* **2000**, *51*, 129–152.

(30) Stern, H. A.; Feller, S. E. Calculation of the dielectric permittivity profile for a nonuniform system: application to a lipid bilayer simulation. *J. Chem. Phys.* **2003**, *118*, 3401–3412.

(31) Spassov, V. Z.; Yan, L.; Szalma, S. Introducing an implicit membrane in Generalized Born/Solvent Accessibility continuum solvent models. *J. Phys. Chem. B* **2002**, *106*, 8726–8738.

(32) Lazaridis, T. Effective energy function for proteins in lipid membranes. *Proteins* **2003**, *52*, 176–192.

(33) Im, W.; Feig, M.; Brooks, C. L. An implicit membrane generalized born theory for the study of structure, stability, and interactions of membrane proteins. *Biophys. J.* **2003**, *85*, 2900–2918.

(34) Sigalov, G.; Scheffel, P.; Onufriev, A. Incorporating variable dielectric environments into the generalized Born model. *J. Chem. Phys.* **2005**, *122*, 094511:1−15.

(35) Ulmschneider, M. B.; Ulmschneider, J. P.; Sansom, M. S. P.; Di Nola, A. A generalized Born implicit membrane representation compared to experimental insertion free energies. *Biophys. J.* **2007**, *92*, 2338–2349.

(36) Sengupta, D.; Smith, J. C.; Ullmann, G. Partitioning of side-chain analogues in a five-slab membrane model. *Biochim. Biophys. Acta* **2008**, *1778*, 2234–2243.

(37) Gallicchio, E.; Levy, R. M. AGBNP: an analytic implicit solvent model suitable for Molecular Dynamics simulations and high-resolution modeling. *J. Comput. Chem.* **2003**, *25*, 479–499.

(38) Seelig, J. Deuterium magnetic resonance: theory and application to lipid membranes. *Q. Rev. Biophys.* **1977**, *10*, 353–418.

(39) Mishima, K. In *Advances in Planar Lipid Bilayers and Liposomes*; Liu Leitmannova, A., Tien, H. T., Eds.; Academic Press: London, 2006; Vol. 3, pp 55−84.

(40) Ramsden, J. J. Molecular orientation in lipid bilayers. *Philos. Mag. B* **1999**, *79*, 381–386.

(41) Ferrarini, A.; Moro, G. J.; Nordio, P. L. Simple molecular model for induced cholesteric phases. *Phys. Rev. E* **1996**, *53*, 681–688.

(42) Ferrarini, A. Shape model for the molecular interpretation of the flexoelectric effect. *Phys. Rev. E* **2001**, *64*, 021710:1−11.

(43) Cestari, M.; Bosco, A.; Ferrarini, A. Molecular field theory with atomistic modeling for the curvature elasticity of nematic liquid crystals. *J. Chem. Phys.* **2009**, *131*, 054104:1−16.

(44) Maier, W.; Saupe, A. A simple molecular-statistics theory of the nematic liquid-crystalline phase. Part I. *Z. Naturforsch. A* **1959**, *14A*, 882–900. Ibidem. A simple molecular-statistics theory of the nematic liquid-crystalline phase. Part II. *Z. Naturforsch. A* **1960**, *15A*, 287−292.

(45) Abramowitz, M.; Stegun, I. A. Handbook of Mathematical Functions; Dover: New York, 1972.

(46) Ferrarini, A.; Luckhurst, G. R.; Nordio, P. L.; Roskilly, S. J. Prediction of the transitional properties of liquid crystal dimers. A molecular field calculation based on the surface tensor parametrization. *J. Chem. Phys.* **1994**, *100*, 1460–1469.

(47) Luckhurst, G. R. In *The Molecular Physics of Liquid Crystals*; Luckhurst, G. R., Gray, G. W., Eds.; Academic: London, 1979; pp 85−119.

(48) Flory, P. J. *Statistical Mechanics of Chain Molecules*; Interscience: New York, 1969.

(49) Richards, F. M. Areas, volumes, packing and protein structure. *Annu. Rev. Biophys. Bioeng.* **1977**, *6*, 151–176.

(50) Sanner, M. F.; Olson, A.; Spehner, J.-C. Reduced surface: an efficient way to compute molecular surfaces. *Biopolymers* **1996**, *38*, 305–320.

(51) Stewart, J. *Calculus*, 4th ed.; Brooks/Cole Publishing Company: Pacific Grove, CA, 1999.

(52) Arfken, G. B.; Weber, H. J. *Mathematical Methods for Physicist*, 4th ed.; Elsevier: Boston, 2005.

(53) Quarteroni, A.; Sacco, R.; Saleri, F. *Numerical Mathematics*; Springer: New York, 2000.

(54) Ollila, O. H. S.; Róg, T.; Karttunen, M.; Vattulainen, I. Role of sterol type on lateral pressure profiles of lipid membranes affecting membrane protein functionality: comparison between cholesterol, desmosterol, 7-dehydrocholesterol and ketosterol. *J. Struct. Biol.* **2007**, *159*, 311–323.

(55) Kupiainen, M.; Falck, E.; Ollila, S.; Niemelä, P.; Gurtovenko, A. A. Free volume properties of sphingomyelin, DMPC, DPPC, and PLPC bilayers. *J. Comp. Theory Nano* **2005**, *2*, 401–413.

(56) Falk, E.; Patra, M.; Karttunen, M.; Hyvönen, M. T.; Vattulainen, I. Lessons of slicing membranes: interplay of packing, free area, and lateral diffusion in phospholipid/cholesterol bilayers. *Biophys. J.* **2004**, *87*, 1076–1091.

(57) *CRC Handbook of Chemistry and Physics*, 85th ed.; Lide, D. R., Ed.; CRC: Boca Raton, FL, 2004.

(58) Frisch, M. J. *Gaussian 03*, revision C.02; Gaussian, Inc.: Wallingford CT, 2004.

(59) Bondi, A. Van der Waals volumes and radii. *J. Phys. Chem.* **1964**, *68*, 441–451.

(60) Jorgensen, W. L.; Maxwell, D. S.; Tirado-Rives, J. Development and testing of the OPLS all-atom force field on conformational energetics and properties of organic liquids. *J. Am. Chem. Soc.* **1996**, *118*, 11225–11236.

(61) Feig, M.; Im, W.; Brooks, C. L. Implicit solvation based on generalized Born theory in different dielectric environments. *J. Chem. Phys.* **2004**, *120*, 903–911.

(62) Harroun, T. A.; Katsaras, J.; Wassall, S. R. Cholesterol hydroxyl group is found to reside in the center of a polyunsaturated lipid membrane. *Biochemistry* **2006**, *45*, 1227–1233.

(63) Gliss, C.; Randel, O.; Casalta, H.; Sackmann, E.; Zorn, R.; Bayerl, T. Anisotropic motion of cholesterol in oriented DPPC bilayers studied by quasielastic neutron scattering: the liquid-ordered phase. *Biophys. J.* **1999**, *77*, 331–340.

(64) Bennett, W. F. D.; MacCallum, J. L.; Hinner, M. J.; Marrink, S. J.; Tieleman, D. P. Molecular view of cholesterol flip-flop and chemical potential in different membrane environments. *J. Am. Chem. Soc.* **2009**, *131*, 12714–12720.

(65) Kučerka, N.; Marquardt, D.; Harroun, T. A.; Nieh, M.-P.; Wassall, S. R.; Katsaras, J. The functional significance of lipid diversity: orientation of cholesterol in bilayers is determined by lipid species. *J. Am. Chem. Soc.* **2009**, *131*, 16358–16359.

(66) Guo, W.; Kurze, V.; Huber, T.; Afdhal, N. H.; Beyer, K.; Hamilton, J. A. A solid-state NMR study of phospholipid-cholesterol interactions: sphingomyelin-cholesterol binary system. *Biophys. J.* **2002**, *83*, 1465–1478.

(67) Dufourc, E. J.; Parish, E. J.; Chitrakorn, S.; Smith, I. C. P. Structural and dynamical details of the cholesterol-lipid interaction as revealed by deuterium NMR. *Biochemistry* **1984**, *23*, 6062–6071.

(68) In the experiments reported in ref 67, the magnetic field was perpendicular to the bilayer normal.

(69) Pavanello, M.; Mennucci, B.; Ferrarini, A. Quantum-mechanical studies of NMR properties of solutes in liquid crystals: a new strategy to determine orientational order parameters. *J. Chem. Phys.* **2005**, *122*, 064906:1−9.

CT100210U